Misan Journal of Engineering Sciences ISSN: 2957-4242
Vol. 5, No. 1, 28 June 2026 ISSN-E: 2957-4250

Decoupling MIMO of Planar Array of Circular Microstrip Antenna for Wireless Applications

Rusel Waheed Laftah[1*], Ahmad H. Abood Al-Shaheen[1]

[1] *Physics Department, College of Science, University of Misan, 62001, Iraq*
**Corresponding author E-mail: rusellaftah@gmail.com*

(Received 1 Dec 2025, Revised 19 Jan 2025, Accepted 1 Feb 2025)

Abstract: This paper describes the creation and simulation of a circular patch antenna array designed for 5.8 GHz operation. The array incorporates three inset-fed microstrip circular patch antennas for beamforming, which helps to reduce the substantial path loss that exists in high-data-rate mm-5G mobile station environments. The configuration consists of three circular patch antenna arrays with separate strip line feeds. In the proposed design, a 7.2 mm-diameter circular patch is placed. To model the antenna array, a FR-4 substrate with a relative permittivity (εr) of 4.4 was employed. Strip line feeding techniques were applied, and the substrate's dimensions are 27 x 67 x 1.6 mm³. The acquired bandwidth is excellent for WLAN applications because it spans frequencies between 5.15 GHz and 6.56 GHz. Over the stipulated bandwidth, the measured gain reaches 4.1 dB with an input impedance of around 50 Ω. Strong agreement was established between the simulated results and experimental data. The design and simulation method made use of the Finite Element Method (FEM)-based High Frequency Structural Simulation (HFSTM) tool.

Keywords: Array Microstrip Antenna; Circular patch; 5G; MIMO

1. Introduction

The advent of fifth-generation (5G) technology marks a significant turning point in the development of wireless communication, bringing with it an era characterized by previously unheard-of data speeds, incredibly low latency, and connectivity that transcends conventional network boundaries. By enabling cutting-edge applications like augmented reality, autonomous driving, and ubiquitous machine-type communications, this new generation of mobile networks is predicted to completely transform a number of industries (A. A. Solyman,2022). But in order to fully utilize 5G, a number of issues need to be resolved, with advancements in antenna design being particularly important. The use of millimeter-wave (mmWave) frequencies, especially in the 28 GHz and 38 GHz bands, is a key component of 5G. mmWave frequencies are crucial for satisfying the growing demand for increased data speed and better connection because of their wide bandwidth (J. Li, Y. Niu,2022). However, there are drawbacks to using these high frequencies, including greater sensitivity to physical obstructions and increased atmospheric attenuation. Notwithstanding these challenges, considerable research and development efforts have been directed toward utilizing mmWave bands for 5G applications due to the promise to provide extremely high data rates and low latency (P. Loktongbam,2023), (H. Askari,2022). Regulatory agencies like as the Federal Communications Commission (FCC) have defined pioneer frequency bands for 5G networks, which are focused around 28 GHz and 38 GHz and encompass ranges like 26.5–29.5 GHz, 27.5–28.35 GHz, and 37–40 GHz, in acknowledgment of their strategic relevance. The overarching goal of delivering operators dependable, fast, high-bandwidth connectivity with minimal latency is in accordance with these allowances.

DOI: https://doi.org/10.61263/mjes.v5i1.240

Both the FCC and the EU have designated several frequency bands for 5G deployment under their regulatory frameworks, mostly in the Ka-band spectrum (26–40 GHz). The 26 GHz band (24.25–27.5 GHz), the 28 GHz band (27.5–28.35 GHz), and the 38 GHz band (37–40 GHz) are notable allocations. Other bands include the 24 GHz range (24.25–24.45 GHz, 24.75–25.25 GHz), the 29 GHz band (29.1–29.25 GHz), and the 32 GHz band (31.4– 33.8 GHz) (S. Ramanathan,2024)- (Khabba,2022). One of the most important aspects of designing 5G wireless networks is using multiple-input multiple-output (MIMO) antenna systems with wideband performance (Zhiqiang,2022). This technology is essential for boosting spectrum efficiency, increasing channel capacity, and increasing data throughput. MIMO systems are valuable in 5G designs because they can accomplish these advantages without requiring more transmission power by taking use of the wireless channel's multipath features (S. H. Kiani 2023). MIMO antennas operating at 28/38 GHz have been the subject of extensive research, indicating its significance for mmWave communication in 5G. A compact planar MIMO antenna array with an inset-fed design specifically designed for 5G applications at 28 GHz and 38 GHz was presented by Rafique et al (Nauman,2021).

This design, which measures 41.5×10×0.8 mm^3, has a peak gain of 5.7 dB and bandwidths of 1.39 GHz and 3.33 GHz for the corresponding bands. A four-element MIMO antenna array with a 110×55 mm^2 size was created by (Marzouk,2019). They were able to accomplish dual-band operation, robust port isolation, and maximum gains of 7.95 dB and 8.27 dB by integrating inverted I-shaped slots into the main patch. Raheel and associates. A 4x4 MIMO antenna with an excellent minimum port isolation of 28 dB was proposed by (K.Raheel,2021) for 5G applications working at both 28 GHz and 38 GHz. At 28 GHz and 38 GHz, this design achieved gains of 7.1 dB and 7.9 dB, respectively. A 79.4×9.65 mm^2 MIMO antenna with a maximum gain of 9 dB and bandwidths of 3.42 GHz and 1.45 GHz for each frequency band was constructed by(Farahat 2021). A 28 GHz tiny dual-port single-element MIMO antenna with a peak gain of 6.9 dB and a 0.4 GHz bandwidth was published by (Usman,2021). The antenna measures 33×27.5×0.76 mm^3. These studies' design processes are usually based on conventional techniques, while performance optimization relies heavily on parametric analysis. Despite their effectiveness, these traditional approaches can be labor- and time-intensive. Rather, artificial intelligence techniques such as radial basis function neural networks (RBFNN) (M. Wang, 2008)–(Aneesh, 2012), adaptive neuro- fuzzy inference systems (ANFIS) (Sellak, 2023), and artificial neural networks (ANN) (Sellak, 2022)–(Ara, 2024) offer ways to expedite the design process and boost efficiency by leveraging computational learning capabilities. There are advantages and disadvantages to the expansion of various frequency bands in 6G networks, ranging from millimeter- wave to terahertz.. By creating a MIMO antenna array especially tailored for the difficult 28 GHz and 38 GHz frequency bands, this research explores the cutting-edge subject of mmWave communication. In addition to offering insights into important advances required to fully exploit the potential of 5G mmWave technology, the work attempts to address the inherent problems of antenna design for the mmWave spectrum.

2. Material and Method

2.1 Single Patch Antenna Design

The top view of single inset feed circular patch antenna depicted in Fig. 1. The antenna is intended to function at a 5.8 GHz resonant frequency. Strip line feeding is used because it makes input impedance matching easier by varying the feed position. Achieving adequate impedance matching is vital for attaining the desired bandwidth; otherwise, the antenna’s effectiveness would be impaired. The substrate thickness is kept as low as possible to guarantee the best bandwidth, adhering to the following rule: $0.003\lambda o < h < 0.05\lambda o$. dielectric material of FR4-Epoxy is utilized as the substrate because of its low relative permittivity ,which is useful since lower permittivity leads to higher bandwidth. In the antenna structure, the patch and strip line feed are placed on the top layer, the substrate forms the middle layer, and the ground plane is at the bottom. At the dominant TM11 mode the effective patch radius is calculated from [Balanis, C.A. (2016)]. Antenna Theory: Analysis and Design. 4th ed. Hoboken, New Jersey Wiley, pp.814–823. Chapter 14.3 Circular Patch.

$$a = \frac{F}{\left\{1+\frac{2h}{\pi S_r F\left[\ln(\frac{\pi F}{2h}+1.7726\right]}\right\}^{\frac{1}{2}}} \quad (1)$$

Where

$$F = \frac{8.791 \times 10^9}{f_r\sqrt{S_r}}$$

Due to the fringing field, the effective radius is given by

$$a_e = a\left\{1 + \frac{2h}{\pi a S_r}\left[\ln\left(\frac{\pi a}{2h} + 1.7726\right)\right]\right\}^{\frac{1}{2}} \quad (2)$$

Where

fr = Resonant Frequency of Circular Patch Antenna εr = Substrate Relative Permittivity
h = Substrate Height
a = Physical Radius of the Patch
*a*e = Effective Radius

This layout represents a typical patch antenna powered by a microstrip line. The feed line is designed with a width of 0.5 mm, and a characteristic impedance of 50 ohms is maintained. As shown in Fig. 1, according to eq.(1) and eq.(2), the proposed geometry features a circular microstrip patch with a radius of 7.2 mm. To achieve 50 W input impedance, two symmetrical inset are introduced into the patch, each dimension is 1 mm in length and 0.5 mm in width.

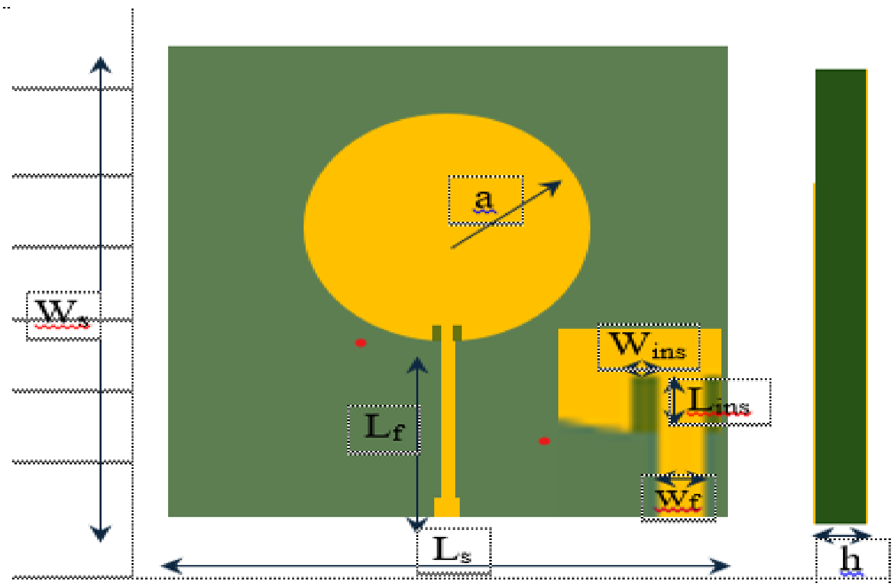

Fig. 1. The geometry of microstrip patch antenna

The dimensions of the proposed antenna are listed in Table 1.

Table 1.: Proposed antenna dimensions (all in mm)

Parameter	Value	Parameter	Value
Ws	27	Ls	27
a	7.2	Wf	0.5
Lf	9.2	Wins	0.5
Lins	1	h	1.6

The HFSS, a structural simulator based on the Finite Element Method (FEM), was used.

2.1.1 Simulation results of a single circular patch antenna

After simulation the proposed antenna using HFSS as a tool the results target such as reflection coefficient, VSWR, Zin, gain and directivity are examined, the first result is the S11 parameter as shown in Fig.2. The bandwidth is obtained with the above dimension of patch and the substrate is about 1.27 GHz around the central frequency 5.8 GHz below −10 dB. Indicating good impedance matching (extremely low reflected power), accomplished proving that the antenna also operates very well in a broader bandwidth around the center frequency as indicated in Fig.4. The antenna is well-matched at 5.8 GHz, which presumably matches to the target C band for WLAN applications. As demonstrated in Fig. 2.

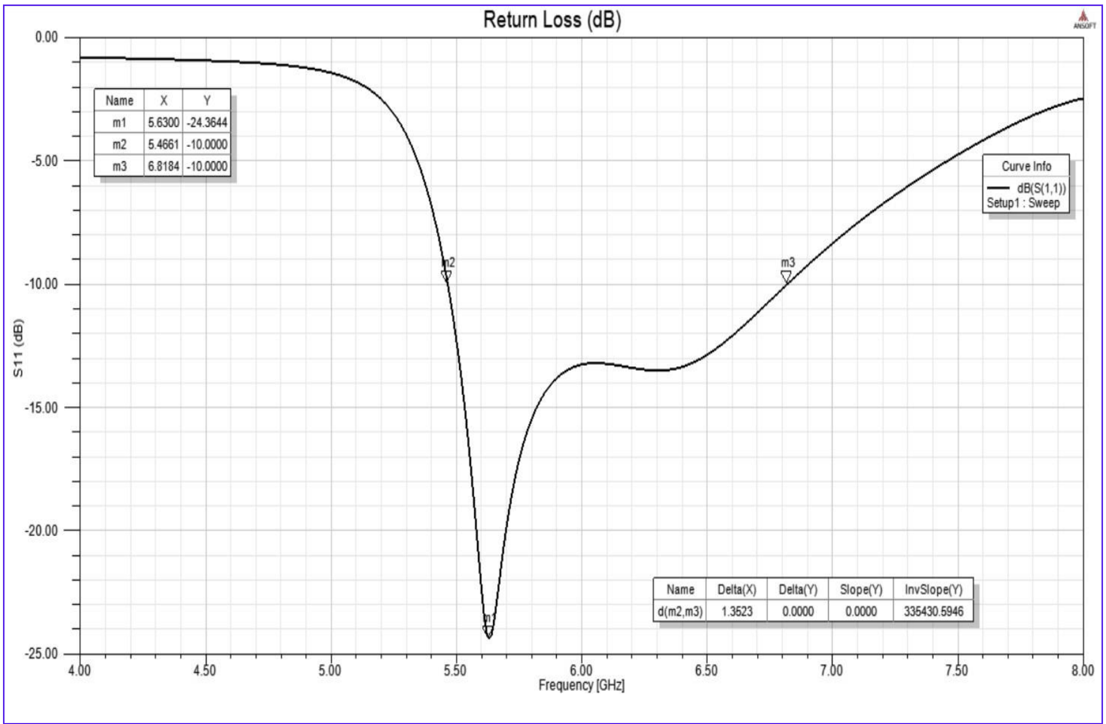

Fig. 2. Reflection coefficients for the single element antenna

In Fig. 3, was found that the shape is non-circular, indicating that the radiation is not uniform in all directions. The radiation pattern shows the presence of lobes, which suggests that the antenna directs energy preferentially in the upward direction.

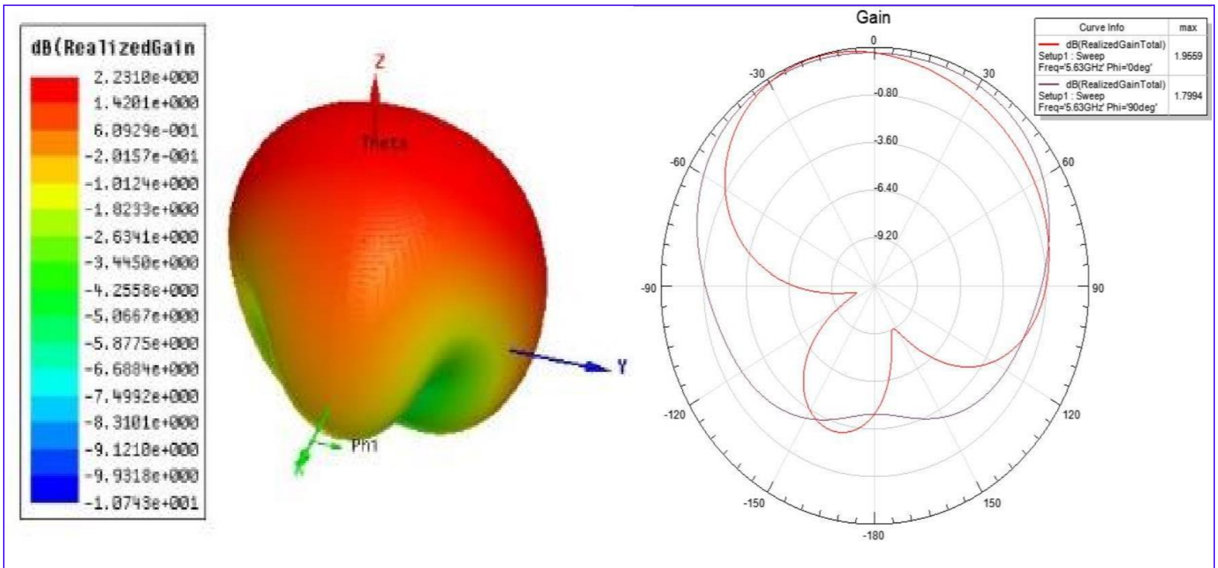

Fig. 3. Radiation Pattern of the Single Antenna

2.2 Three Element Circular Patch Antenna Array Design

The geometry of three elements circular patch antenna array is shown in Fig. 4. This geometry consists of three previous designed low profile inset feed circular patch antennas each of them has the same optimized dimensions shown in Table1.

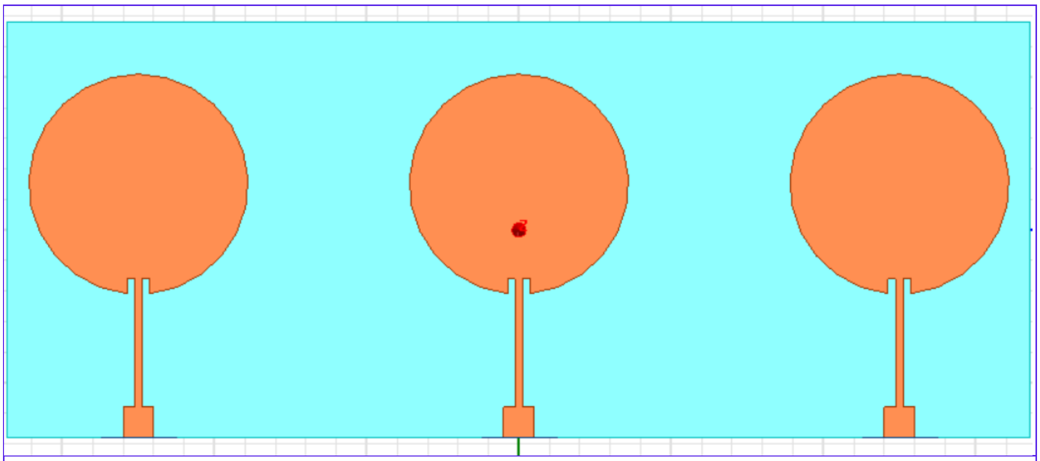

Fig. 4. Three-element circular patch antenna array design

Three ports (50–100Ω) for each antenna and three transition micro strip feed lines having length equal quarter of operating wavelength (λ/4). Antenna design and simulation were carried out in Finite Element Method (FEM) based High Frequency Structural Simulation (HFSSTM) tool.

2.2.1 Simulation Results of Circular Patch Antenna Array

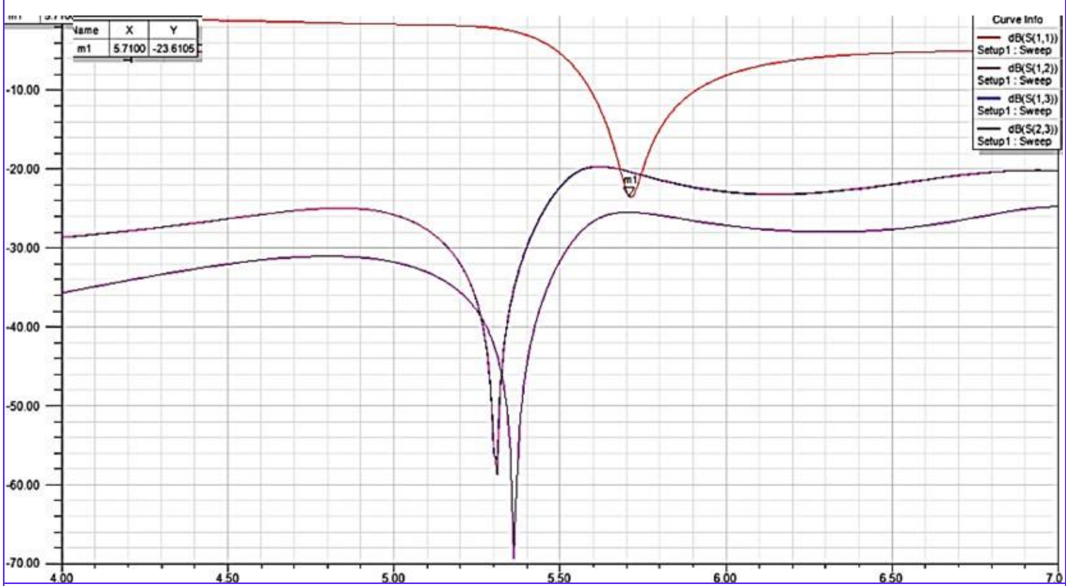

Fig. 5. Simulation of array

The scattering parameter analysis results showed that the studied antenna operates with high efficiency at 5.71 GHz, where the reflection coefficient (S11) at this frequency was approximately −23.6 dB. This value indicates that the amount of power reflected from the antenna is relatively low. The coupling coefficient between the antenna elements was analyzed by studying the transmission parameters between the ports (S-parameters); at 5.71 GHz, it was less than−20 dB.

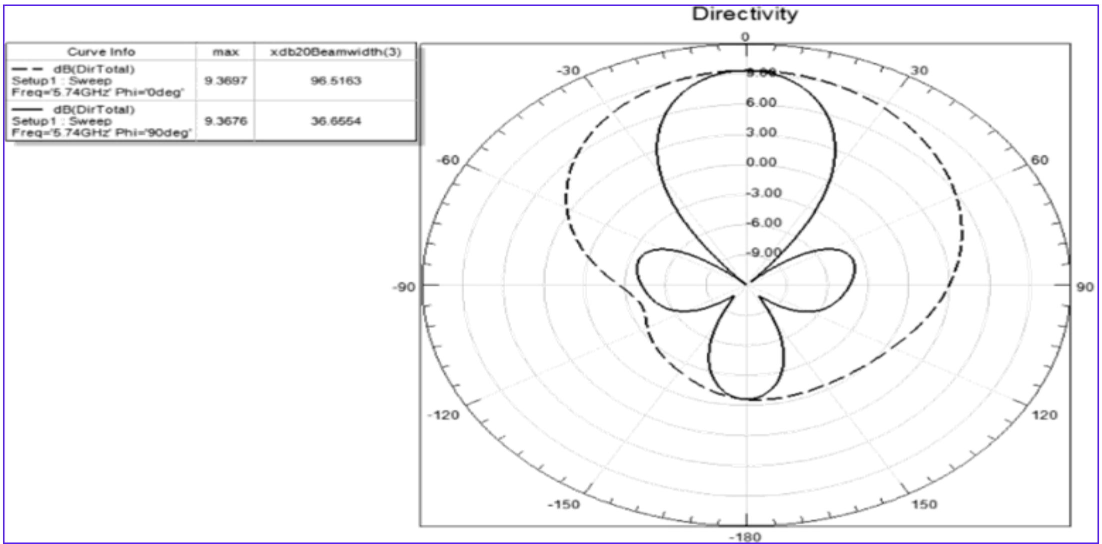

Fig. 6. Radiation Pattern of the Array

The figure illustrates the radiation pattern of the antenna at 5.8 GHz in two different φ-plane cuts, where the red curve represents **φ = 0°** (the vertical plane) and the green curve represents φ = 90° (the horizontal plane). From the plot, it can be observed that the radiation in the vertical plane is more focused and directional, with a peak radiation level of approximately 29 dB**,** indicating that the antenna exhibits relatively good directivity and efficiently concentrates energy in a specific direction. In the horizontal plane, however, the radiation pattern appears to be distributed over multiple directions with a comparatively lower radiation level. Additionally, the side lobes in both planes are low, which indicates reduced unwanted radiation and, consequently, improved antenna efficiency.

The experimental results of the array demonstrated the presence of mutual coupling between the three circular antennas. To reduce this mutual coupling and achieve better performance of the radiated signal from the antenna, a new array was designed with the same dimensions as the previous one, incorporating internal slots in the design between the antennas to minimize the mutual coupling as shown in the Fg. 7**.** The dimensions of these designed slots can also be seen in Fig. 8.

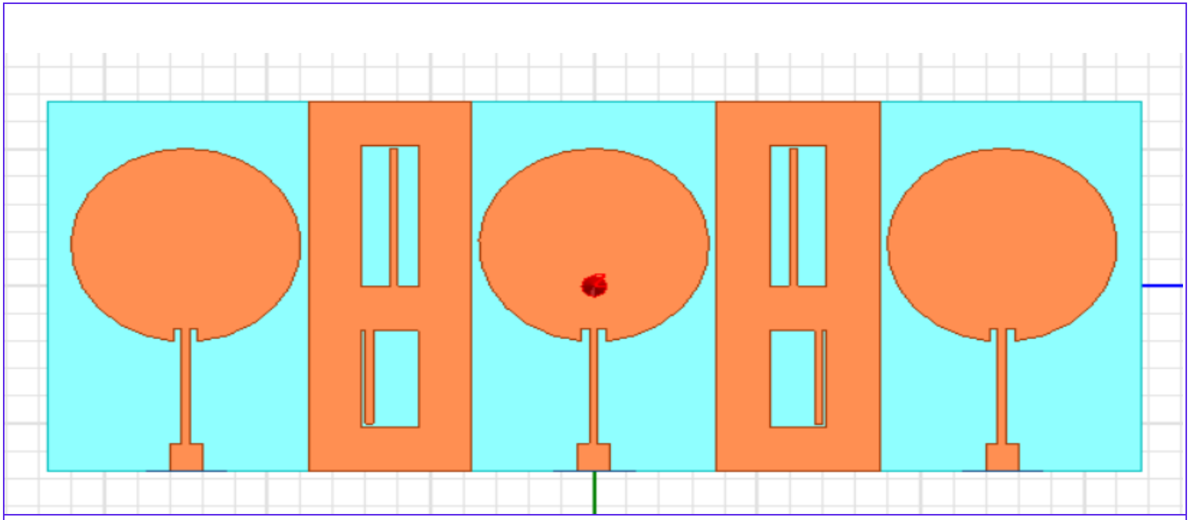

Fig. 7. The Array with slot

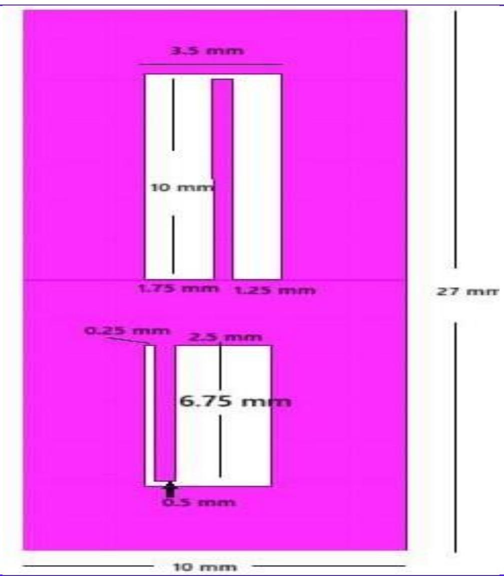

Fig. 8. The dimensions of the slots

2.3 Simulation Results

The antenna array is well matched at 5.8290 GHz with very low reflection (S11 = −39.7 dB), which is a very good performance. The transmission coefficient (S21) shows that the device allows decent signal coupling within the 5.68–6.12 GHz range (within −10 dB), which is typical for defining the operating bandwidth. This implies the structure (perhaps an antenna or filter) is operational around 5.8–6.1 GHz, depending on whether you are focused on matching (S11) or transmission (S21). S(2,3) curve appears to be relatively high in dB (less negative), suggesting low mutual coupling or weak transmission between those two ports good for MIMO/antenna isolation if that's the goal.

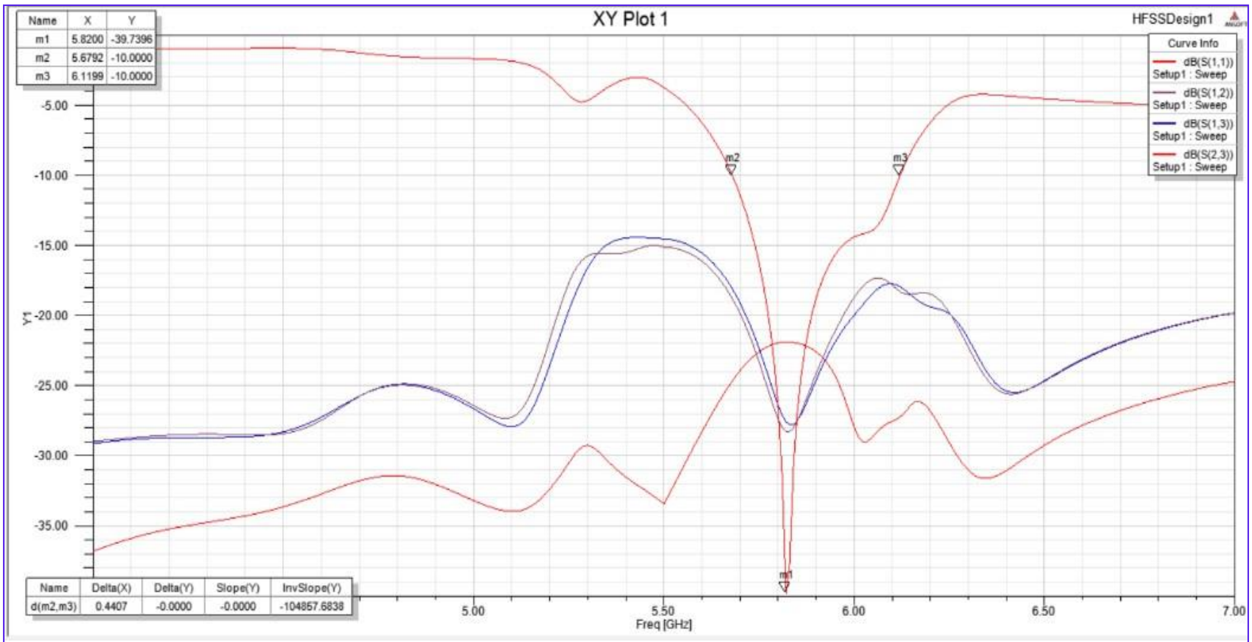

Fig. 9. simulation results of circular patch antenna array

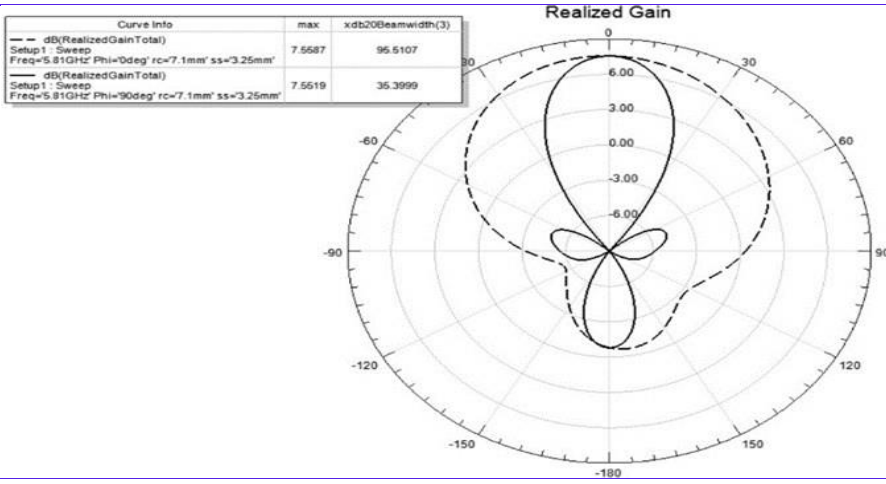

Fig. 10. Radiation pattern

Thus, we achieved excellent results for the proposed antenna, with high radiation efficiency, high directivity, and a very low mutual coupling coefficient.

3. Result and Discussion

3.1 Experimental Results

The model was implemented at the Scientific Research Authority of the Ministry of Science and Technology, and the return loss and Voltage Standing Wave Ratio (VSWR) were measured using a Vector Network Analyzer (VNA) (Vector Star Analyzer), as shown in the Fig.10.

Fig. 11. Vector Star VNA

In order to analyze and improve the performance of contemporary antennas and RF components, the Anritsu VectorStar VNA is an innovative analytical platform that combines broad frequency coverage, high accuracy, quick measurement speed, and a great deal of flexibility. Depending on the model, the series covers frequency ranges from 70 kHz to 70/110/125/145/220 GHz. It offers remarkable capabilities in discriminating weak signals thanks to a dynamic range of 124 dB at 110 GHz, or up to 109 dB at 110 GHz and 102 dB at 220 GHz, depending on the type.The VectorStar- class VNA is widely used to measure S-parameters (such as S11 and S21) to evaluate antenna matching and transmission efficiency (return loss, VSWR). It is highly suitable for analyzing antennas at high frequencies and in various configurations such as HFSS simulations, R&D, and industrial testing.

3.1.1 The Experimental Results for A Single Patch Antenna

We notice that the results of the single circular antenna design using the HFSS simulation program are identical to the results obtained in practice. It is also observed that there is a slight shift in the central frequency as well as in the frequency bandwidth. This is attributed to the fact that the design choices within the simulation program assume an ideal condition for the entire design and do not take welding areas into consideration.

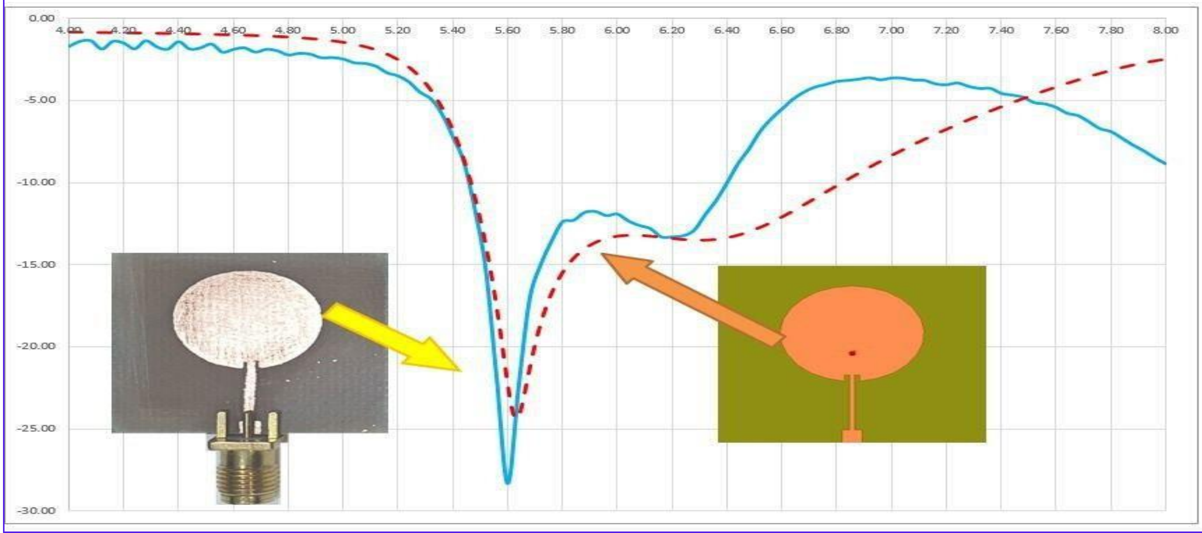

Fig. 12. The Experimental results For Single Patch Antenna

3.1.2 The Experimental results For Circular Patch Antenna Array

In Fig.12, the reflection coefficient results (S11, S22, S33) for three circular antennas inside the array are given, along with a comparison between the simulated results and the experimental results.The simulated results are shown by solid lines, and the experimental findings are shown by dashed lines. We discover that all three antennas show a distinct resonance response close to the intended frequency of 5.8 GHz. This implies excellent impedance matching in this frequency region. The simulated and experimental values show a slight shift in the resonant frequency of approximately 0.05–0.1 GHz. This shift is expected due to variations in the dielectric constant (εr) in practical implementation, additional loss in the conductor or dielectric material, and potential manufacturing or soldering process errors. The three antennas are appropriate for MIMO antenna array applications in the WLAN or 5G sub-6 GHz band since they all function at about the same frequency range (around 5.8 GHz).

We conclude that the theoretical results match the practical results for every model that was worked on. We arrive at the final conclusion that the proposed antenna design possesses good isolation and excellent radiation efficiency, making it suitable for MIMO applications in the proposed 5-6 GHz frequency band within wireless communication applications such as WiFi and other range-limited applications.

4. Conclusions

From the above, we can deduce the theoretical (simulation) results for the MIMO matrix parameters as follows Regarding the Envelope Correlation Coefficient (ECC), it was less than 0.05, indicating a high level of independence between the transmission channels. The Diversity Gain (DG) results were very close to 10 dB, confirming the system's efficiency in resisting fading. The Channel Capacity Loss (CCL) results were less than 0.3 bit/s/Hz, which is within acceptable limits for modern MIMO systems. Finally, the Total Active Reflection Coefficient (TARC) was mostly below -10 dB within the frequency band, indicating effective mutual coupling. We conclude that the proposed antenna design has good isolation and excellent radiation efficiency, making it suitable for MIMO applications in the proposed 5-6 GHz frequency band for wireless communication applications such as WiFi and other applications within this range.

Author Contributions: The authors contributed to all parts of the current study.
Funding: This study received no external funding.
Conflicts of Interest: The authors declare no conflict of interest.

5. Rferences

[1] A. A. Solyman and K. Yahya, "Evolution of wireless communication networks: from 1G to 6G and future perspective," International Journal of Electrical and Computer Engineering, vol. 12, no. 4, pp. 3943-3950, 2022, DOI: http://doi.org/10.11591/ijece.v12i4.pp3943-3950
[2] J. Li, Y. Niu, H. Wu, B. Ai, S. Chen, Z. Feng, Z. Zhong, and N. Wang, "Mobility Support for Millimeter Wave Communications: Opportunities and Challenges," IEEE Communications Surveys & Tutorials, vol. 24, no. 3, pp. 1816–1842, 2022, DOI: 10.1109/COMST.2022.3176802.
[3] P. Loktongbam, D. Pal, A. Bandyopadhyay, and C. Koley, "A brief review on mm-Wave antennas for 5G and beyond applications,"IETE Technical Review, vol. 40, no. 3, pp. 397–422, 2023. DOI:10.1080/02564602.2022.2121771
[4] L. Sellak, A. Khabba, S. Chabaa, S. Ibnyaich, A. Sarosh, A. Zeroual, and A. Baddou, "ANFIS-Based 4× 4 Dual Band CircularMIMOAntennaDesignwith Pretty-Small Size and Large Bandwidth for 5 G Millimeter-Wave Applications at 28/38 GHz," Journal of Infrared, Millimeter, and Terahertz Waves, vol. 44, no. 7-8, pp. 551–601, 2023, DOI:10.1007/s10762-023-00924-3
[5] H. Askari, N. Hussain, M. A. Sufian, S. M. Lee, and N. Kim, "A wideband circularly polarized magnetoelectric dipole antenna for 5G millimeter-wave communications," Sensors, vol. 22, no. 6, p. 2338, 2022. https://doi.org/10.3390/s22062338
[6] S. Ramanathan and A. B. Maria, "A compact four-element MIMO antenna for 5 G millimeter-wave (37–39 GHz) applications," Journal of Infrared, Millimeter, and Terahertz Waves, vol. 45, no. 7–8, pp. 604–620, 2024, doi:10.1007/s10762-024-00990-1. A Compact Four-Element MIMO Antenna for 5 G Millimeter-Wave (37–39 GHz) Applications | Journal of Infrared, Millimeter, and Terahertz Waves
[7] Khabba, J. Amadid, S. Ibnyaich, and A. Zeroual, "Pretty-small four-port dual-wideband 28/38 GHz MIMO antenna with ro bust isolation and high diversity performance for millimeter-wave 5G wireless systems," Analog Integrated Circuits and Signal Processing, vol. 112, no. 1, pp. 83–102, 2022, https://doi.org/10.1007/s10470-022-02045-8.
[8] Z. Xu, World Of 5g, The-Volume 4: Intelligent Transportation. World Scientific, 2022 World Of 5g, The - Volume 4: Intelligent Transportation: Xu, Zhiqiang: 9789811244162: Amazon.com: Books
[9] S. H. Kiani, H. S. Savci, M. E. Munir, A. Sedik, and H. Mostafa, "An Ultra-Wide Band MIMO Antenna System with Enhanced Isolation for Microwave Imaging Applications," Micromachines, vol. 14, no. 9, p. 1732, 2023, DOI:10.3390/mi14091732.
[10] U.Rafique,S.Agarwal, N.Nauman, H.Khalil, and K. Ullah, "Inset-fed planar antenna array for dual-band 5G MIMO applications," Progress In Electromagnetics Research C, vol. 112, pp. 83–98, 2021, doi:10.2528/PIERC21021302.
[11] H. M. Marzouk, M. I. Ahmed, and A. H. A. Shaalan, "Novel dual-band 28/38 GHz MIMO antennas for 5G mobile applications," Progress In Electromagnetics Research C, vol. 93, pp. 103–117, 2019,

doi:10.2528/PIERC19032303.
[12] K.Raheel, A. Altaf, A. Waheed, S. H. Kiani, D. A. Sehrai, F. Tubbal, and R. Raad, "E-shaped H-slotted dual band mmWave antenna for 5G technology," Electronics, vol. 10, no. 9, p. 1019, 2021 https://doi.org/10.3390/electronics10091019.
[13] A. E. Farahat and K. F. Hussein, "Dual-band (28/38 GHz) MIMO antenna system for 5G mobile communications with efficient DoAestimation algorithm in noisy channels," The Applied Computational Electromagnetics Society Journal (ACES), vol. 36, no. 3, pp. 282–294, 2021, doi: 10.47037/2020.ACES.J.360308. Dual-band (28/38 GHz) MIMO Antenna System for 5G Mobile Communications with Efficient DoA Estimation Algorithm in Noisy Channels | ScienceGate
[14] M.Usman, E. Kobal, J. Nasir, Y. Zhu, C. Yu, and A. Zhu, "Compact SIW fed dual-port single element annular slot MIMO antenna for 5G mmWave applications," IEEE Access, vol. 9, pp. 91995–92002, 2021, DOI:10.1109/ACCESS.2021.3091835
[15] L. Sellak, L. Aguni, S. Chabaa, S. Ibnyaich, A. Zeroual, and A. Baddou, "Modeling and Designing of a Compact Single Band PIFA Antenna for Wireless Application Using Artificial Neural Network," Wireless Personal Communications, vol. 127, no. 4, pp. 3097–3117, 2022, doi: 10.1007/s11277-022-09912-7. Modeling and Designing of a Compact Single Band PIFA Antenna for Wireless Application Using Artificial Neural Network Wireless Personal Communications
[16] L. Aguni, A. El Yassini, S. Chabaa, S. Ibnyaich, and A. Zeroual, "Design of a symmetric CPW-fed patch antenna for WLAN/WIMAX applications using ANN," Wireless Personal Communications, vol. 115, no. 1, pp. 439–456, 2020, doi: 10.1007/s11277-020-07580-z. Design of a Symmetric CPW-Fed Patch Antenna for WLAN/WIMAX Applications Using ANN | Wireless Personal Communications.
[17] S. Ara and P. K. Nunna, "Gain and radiation pattern enhancement using ANN-based reflector antenna for full 5G Sub-6GHz applications," International Journal of Advanced Technology and Engineering Exploration, vol. 11, no. 114, pp. 644–667, 2024, doi: 10.19101/IJATEE.2023.10101979. ACCENTS Journals
[18] M.Wang,S.Yang,S.Wu,andF.Luo, "ARBFNNapproachforDoAestimationofultra wideband antenna array," Neurocomputing, vol. 71, no. 4-6, pp. 631–640, 2008, DOI: 10.1016/j.jneumeth.2007.08.023
[19] J. Dong, Y. Li, and M. Wang, "Fast multi-objective antenna optimization based on RBF neural network surrogate model optimized by improved PSO algorithm," Applied Sciences, vol. 9, no. 13, p. 2589, 2019, doi:10.3390/app9132589. https://doi.org/10.3390/app9132589
[20] M. Aneesh, J. Ansari, A. Singh, S. Verma, "RBF neural network modeling of rectangular microstrip patch antenna," in 2012 Third International Conference on Computer and Communication Technology, IEEE, 2012, pp. 241–244, https://doi.org/10.1109/ICCCT.2012.56
[21] L. Sellak, A. Khabba, S. Chabaa, S. Ibnyaich, A. Baddou, and A. Zeroual, "Adaptive Neuro-Fuzzy Inference System-Based Ap proach to Design a Multi-Band PIFA Antenna for Wireless Applications," in 2023 IEEE 3rd International Maghreb Meeting of the Conference on Sciences and Techniques of Automatic Control and Computer Engineering (MI-STA), IEEE, 2023, pp. 732–737, DOI: 10.1109/MI-STA57575.2023.10169336.

ISSN: 2957-4242
ISSN-E: 2957-4250